

## Imperative role of particulate matter in innate immunity during RNA virus infection

— [Source link](#) 

[Richa Mishra](#), [K Pandikannan](#), [S. Gangamma](#), [Ashwin Ashok Raut](#) ...+2 more authors

**Institutions:** [Indian Institute of Science](#), [National Institute of Technology, Karnataka](#), [Indian Council of Agricultural Research, Osaka University](#)

**Published on:** 29 Mar 2020 - [bioRxiv](#) (Cold Spring Harbor Laboratory)

**Topics:** [Influenza A virus subtype H5N1](#), [Innate immune system](#), [Immune system](#) and [Virus](#)

Related papers:

- [Particulate matter \(PM10\) enhances RNA virus infection through modulation of innate immune responses](#)
- [Influenza A Virus Infection, Innate Immunity, and Childhood](#)
- [Pathogenesis of influenza virus infections: the good, the bad and the ugly](#)
- [The host immune response in respiratory virus infection: balancing virus clearance and immunopathology](#)
- [Innate immune cell suppression and the link with secondary lung bacterial pneumonia](#)

Share this paper:    

View more about this paper here: <https://typeset.io/papers/imperative-role-of-particulate-matter-in-innate-immunity-2p8ylsa1o2>

1 **Imperative role of particulate matter in innate immunity during RNA virus infection**

2

3 Richa Mishra<sup>1</sup>, Pandikannan K<sup>1</sup>, Gangamma S<sup>2,3</sup>, Ashwin Ashok Raut<sup>4</sup>, Himanshu Kumar<sup>1,5\*</sup>

4

5 **Affiliations:** 1. Department of Biological Sciences, Laboratory of Immunology and Infectious

6 Disease Biology, Indian Institute of Science Education and Research (IISER) Bhopal, Bhopal -

7 462066, MP, India; 2. National Institute of Technology Karnataka (NITK), Surathkal, Mangaluru

8 - 575025, Karnataka, India; 3. Centre for Water Food and Environment, IIT Ropar, Rupnagar-

9 140001, Punjab, India. 4. Pathogenomics Laboratory, ICAR – National Institute of High Security

10 Animal Diseases (NIHSAD), OIE Reference Laboratory for Avian Influenza, Bhopal - 462021,

11 MP, India; 5. Laboratory of Host Defense, WPI Immunology, Frontier Research Centre, Osaka

12 University, Osaka 5650871, Japan.

13

14

15

16

17

18

19

20

21 **\*Corresponding author:** H Kumar, Department of Biological Sciences, Laboratory of

22 Immunology and Infectious Disease Biology, Indian Institute of Science Education and Research

23 (IISER) Bhopal, AB-3, Room No. 220, Bhopal By-pass Road, Bhauri, Bhopal 462066, MP, India.

24 Tel: +91 755 6691413; Fax: +91 755 669 2392; E-mail: [hkumar@iiserb.ac.in](mailto:hkumar@iiserb.ac.in)

25 **ABSTRACT**

26 Sensing of pathogens by specialized receptors is the hallmark of the innate immune response.  
27 Innate immune response also mounts a defense response against various allergens and pollutants  
28 including particulate matter present in the atmosphere. Air pollution has been included as the top  
29 threat to global health declared by WHO which aims to cover more than three billion people against  
30 health emergencies from 2019-2023. Particulate matter (PM), one of the major components of air  
31 pollution, is a significant risk factor for many human diseases and its adverse effects include  
32 morbidity and premature deaths throughout the world. Several clinical and epidemiological studies  
33 have identified a key link between the PM composition and the prevalence of respiratory and  
34 inflammatory disorders. However, the underlying molecular mechanism is not well understood.  
35 Here, we investigated the influence of air pollutant, PM<sub>10</sub> during RNA virus infections using highly  
36 pathogenic avian influenza (HPAI). We thus characterized the transcriptomic profile of lung  
37 epithelial cell line, A549 treated with PM<sub>10</sub> prior to infection with (HPAI) H5N1 influenza virus,  
38 which is known to severely affect the lung and cause respiratory damage. We found that PM<sub>10</sub>  
39 regulates virus infectivity and enhances overall pathogenic burden in the lung cells. Additionally,  
40 the transcriptomic profile highlights the connection of host factors related to various metabolic  
41 pathways and immune responses which were dysregulated during virus infection. Overall our  
42 findings suggest a strong link between the prevalence of respiratory illness and the air quality.

43

44

45

46 **Keywords:** Particulate Matter (PM<sub>10</sub>), Virus Infection, Infectious Disease, Innate Immunity and  
47 Metabolic Pathways-Related Genes.

## 48 INTRODUCTION

49 Seven million people are estimated to be killed every year by the air pollution according to the  
50 WHO (<http://www.who.int/mediacentre/news/releases/2014/air-pollution/en/>). WHO has  
51 recommended standard permissible level of air contaminants but nearly 80% of the urban cities  
52 are well above the standard permissible level (<https://www.who.int/airpollution/data/cities/en/>).  
53 Alarming rate of air pollution in recent years is known to be linked with increased mortality rate  
54 and affected the global health and economy [1-6]. One of the major components of air pollution is  
55 particulate matter (PM). PM collected from different sources or geographical area may have  
56 different impact on the inflammatory and innate immune responses corresponding to the virus  
57 infection on human health. Airborne PM were considered the hazardous causative determinants of  
58 several diseases such as respiratory, cardiovascular and neurological disorders. These particles are  
59 divided into three main categories on the basis of their diameter: coarse particles, or PM<sub>10</sub>, (with  
60 an aerodynamic diameter between 10 and 2.5 µm); fine particles, or PM<sub>2.5</sub>, (with diameters  
61 < 2.5 µm); and ultrafine particles, or PM<sub>0.1</sub>, (with diameters < 0.1 µm) [7]. Numerous studies  
62 revealed that particulate matter collected from different locations all over the world is strongly  
63 associated with the elevated morbidity and mortality and various diseases [8-13]. Several studies  
64 have attempted to understand the link between PM isolated from heavily populated regions of  
65 India and associated health concerns in term of occurrence of disease [14-19]. Although, most of  
66 the studies were based on the epidemiological data and cross-sectional studies, there were few  
67 studies about involvement of PM in respiratory diseases [20-22], asthma [23], cancer [24-27],  
68 tuberculosis [28, 29] . It has been known that PM can induce innate immunity and can change the  
69 level of cytokines, upon its exposure to the airways of humans [30-33]. PM were readily associated  
70 with respiratory infections such as chronic obstructive pulmonary disease (COPD) [34-37] and it

71 is also reported to be associated with the respiratory syncytial virus (RSV) and influenza virus  
72 infections. [38-41]. Yet these studies are limited to epidemiological, cross-sectional studies [22,  
73 42-44].

74 Here, we isolated and characterized PM<sub>10</sub> from a heavily industrialized city Bengaluru, India and  
75 checked its effect on RNA virus infection. We observed and concluded that PM<sub>10</sub> hijacks the innate  
76 immune system upon viral infection and significantly enhanced the viral replication of the RNA  
77 viruses like new-castle disease virus (NDV), influenza virus - H1N1 (PR8) and H5N1. By  
78 performing RNA sequencing analysis, we found that pre-exposure of PM<sub>10</sub> to the cells  
79 downregulates the anti-viral innate immunity related genes in lung (A549) cells during H5N1  
80 infection. Additionally, we reported the upregulation of some previously unknown metabolism-  
81 related genes by global transcriptomic profile analysis and observed its role during virus infection  
82 as demonstrated by knock down studies of identified genes. These metabolic-related genes play  
83 significant role in promoting viral replication in presence of airborne PM.

## 84 **RESULTS**

### 85 **Physical and chemical characterization of PM<sub>10</sub>**

86 To investigate the airborne particles, precisely known as coarse size particulate matter (PM<sub>10</sub>), that  
87 were collected and used in the study, we performed SEM-EDS analysis of PM<sub>10</sub> collected from  
88 Bengaluru city, India. SEM-EDS techniques decipher the particle shape and chemical  
89 composition. It is a method for high resolution surface imaging using electron beams. SEM-EDS  
90 analysis provided us an understanding about the differences in morphology and elemental  
91 composition of the airborne PM<sub>10</sub> collected samples. To understand the effect of PM<sub>10</sub> on host  
92 cells, we initially characterized the particles through imaging and identified that various shapes  
93 were embedded in the particulate matter. We found different biologically active morphological  
94 features within the particulate matter PM<sub>10</sub> (Fig. 1). These varied characteristic features of PM<sub>10</sub>  
95 consists of biologically active shapes like air ash, spherical, irregular, well-defined, aggregates and  
96 rounded. Next, we investigated the types and concentration of elements present in PM<sub>10</sub> to decipher  
97 the origin in terms of biogenic, geogenic and anthropogenic particles. To this end, we performed  
98 energy dispersive spectroscopy (EDS) analysis and found different concentrations of various  
99 metals. We got different peaks in the spectrum obtained upon analysing the sample at different  
100 points with the pulse of electrons (Supplementary Fig. S1A). The peaks in the spectra correspond  
101 to the presence of different elements particularly metals (% by weight) in the particulate matter  
102 (Supplementary Fig. S1B). Some of the listed metals and non-metals (in traces and/or abundance)  
103 are iron, carbon, oxygen, aluminium, lead, silver, silica, titanium, cadmium, sodium, chloride,  
104 magnesium, copper, zinc, gold, tin, vanadium, chromium, nickel, arsenic, molybdenum, barium,  
105 potassium, sulphur, strontium, manganese, cobalt and selenium.

106

## 107 **Exposure of PM<sub>10</sub> reduces innate immunity upon RNA virus infection**

108 As reported previously, particulate matter or similar substances like smog, diesel exhaust ,cigarette  
109 smoke extract causes activation of the inflammatory responses when comes in contact with host's  
110 airways and lungs [41] . Therefore, characterization of PM<sub>10</sub> prompted us to examine whether  
111 PM<sub>10</sub> can induce any innate immune responses in human lung epithelial carcinoma cells, A549.  
112 Interestingly, we have found that when cells were exposed to PM (II), which correspond equal  
113 volume of PM<sub>10</sub> and DMEM media, type I interferon, IFN $\beta$  (Fig. 2A) and inflammatory cytokine  
114 IL-6 (Fig. 2B) were induced. Furthermore, we performed IFN $\beta$  and ISRE promoter assay after  
115 infection with NDV in presence of PM<sub>10</sub> and found that there was significant reduction in the  
116 promoter activities at the dosage of PM<sub>10</sub> (II) (Fig. 2C). Additionally, we concluded that in  
117 different set of experiments dual treatment of PM<sub>10</sub> and virus infection (NDV) to A549 cells as  
118 shown in schematic representation (Fig. 2D) reduces the mRNA transcript levels of interferon  
119 IFN $\beta$  and cytokine IL-6 (Fig. 2E-F). These findings further prompted us to investigate whether  
120 currently characterized PM<sub>10</sub> is associated with any respiratory diseases because majority of  
121 infectious-respiratory diseases are mainly caused by RNA viruses.

122 Previously, it has been shown that cigarette smoke extract (CSE) affects various regulatory  
123 pathways during rhinovirus (RV) infection using human bronchial cell lines by microarray analysis  
124 [41]. We re-analyse the GEO dataset: GSE27973 in context to our prospective and found that there  
125 are several important cellular machineries associated genes (Supplementary Fig. S2A) were  
126 modulated due to CSE exposure and RV infection. We next analysed the regulation of important  
127 genes involved in diseases particularly influenza (flu) virus infection and key immune signalling  
128 pathways (Supplementary Fig. S2B-D). Gene profile analysis concluded that various antiviral  
129 genes were prominently downregulated upon CSE exposure and RV infection. Here, in current

130 study we used influenza virus infection along with PM<sub>10</sub> treatment in the A549 cells, because  
131 influenza virus infection is severely fatal compared to any other virus that causes respiratory  
132 damage and influenza virus is regularly active upon the evolutionary scale and regarded as one of  
133 the hazardous threats according to WHO to humans. Therefore, to get insights about PM<sub>10</sub> exposure  
134 and highly pathogenic avian influenza infection (HPAI), we treated the A549 cells with PM<sub>10</sub> and  
135 infected them HPAI H5N1 (MOI 2) as shown in schematic representation (Fig. 2G). We observed  
136 that that PM<sub>10</sub> reduces the mRNA expression levels of both IFN $\beta$  and IL-6 in presence of H5N1  
137 infection (Fig. 2H-I), indicating that during pathogenic infection by RNA viruses, particularly  
138 influenza virus, PM<sub>10</sub> reduces the innate immune response in the cells.

139

#### 140 **PM<sub>10</sub> enhances viral replication upon RNA virus infection**

141 Curtailed immune responses upon PM<sub>10</sub> treatment and virus infections: both in case of NDV and  
142 H5N1 influenza virus infections, prompted us to measure the viral load in presence of PM<sub>10</sub>. We  
143 thus demonstrated the experiment of PM<sub>10</sub> exposure and virus infection like NDV, H1N1 (PR-8)  
144 and H5N1 in A459 cells respectively. Using virus-specific primer, it was observed that PM<sub>10</sub>  
145 significantly enhances the viral replication of all the RNA viruses ubiquitously. PM<sub>10</sub> enhances the  
146 virus replication of NDV (Fig. 3A), H5N1 (Fig. 3B) and H1N1 (Fig. 3C). Additionally,  
147 microscopy analysis demonstrates similar results in which GFP tagged NDV was used to infect  
148 the PM<sub>10</sub> pre- exposed cells (Fig. 3D). Increased NDV infection was quantified by measuring the  
149 intensity of GFP signal and number of GFP positive cells (Fig. 3E-F). Furthermore, presence of  
150 PM<sub>10</sub> along with NDV infection induces cell death as an additional detrimental effect on cells,  
151 quantified by the trypan blue assay (Fig. 3G). Altogether, our results conclude that PM<sub>10</sub> enhances  
152 the viral replication pertaining to lower immune responses.



153 **RNA-Seq analysis of H5N1 infected cells in presence of PM<sub>10</sub>**

154 PM<sub>10</sub> enhances the viral replication and suppress the immune responses. To further understand the  
155 global outcome of immune responses within the human cell and to dissect the mechanism about  
156 the current physiological effect, we performed RNA sequencing to profile the overall changes in  
157 the host genes and cellular pathways upon PM<sub>10</sub> treatment and HPAI H5N1 infection. Schematic  
158 workflow of the experiment and transcriptomic sequencing shown in Fig. 4A. Differential  
159 expression of host genes analysis was performed between PM<sub>10</sub>-treated\_H5N1-infected and  
160 subsequently mock-treated\_H5N1-infected samples. Differentially expressed genes were marked  
161 in red and other regulated genes which were altered more than 1.5 fold were marked in blue,  
162 altogether they were represented by a volcano plot (Fig. 4B). Next, to understand the overall  
163 cellular changes, gene ontology analysis was performed through DAVID tool to obtained the  
164 enriched biological terms from the top differentially expressed genes with the fold change between  
165  $-1.5 < \log FC > 1.5$ . The top enriched pathways were depicted in bubble plot and circle plot  
166 generated through R package GOplot (Fig. 4C). Herewith, bubble plot represents the significant  
167 enriched ontology terms like biological process (BP), cellular components (CC) and molecular  
168 functions (MF). Circle plot represents the connection between these significantly enriched  
169 ontology terms and the status of genes contributing to each ontology terms. Additionally, the chord  
170 plot represents the connection of common significant differentially expressed genes with the  
171 significant enriched ontology terms (Supplementary Fig. S3A). Gene ontology analysis revealed  
172 that significantly down-regulated genes during H5N1 infection in presence of PM<sub>10</sub> were involved  
173 majorly in various immune signaling pathways and innate immune responses, in accordance with  
174 our experimentally validated results. On contrary, comprehensive analysis revealed that  
175 significantly up-regulated genes were majorly involved in various metabolic pathways. To test

176 this, pathway enrichment analysis was performed through DAVID tool and top enriched pathways  
177 of differentially expressed genes with  $-1.5 < \log FC < 1.5$  were represented by the chord plot  
178 depicting the network between significant differentially expressed genes and their enriched  
179 pathways. Additionally, circle plot depicts the connection of top enriched pathways with the status  
180 of the genes contributing to the pathway represented by their logFC and Z-score (Fig. 4D).  
181 Furthermore, representative of up-regulated genes from significantly regulated metabolic  
182 pathways were validated by qRT-PCR analysis and found the enhanced mRNA expression levels  
183 of VIPR1, CYP1A1, ALDH1A3 and PPP1R14A genes upon H5N1-infection in A549 cells in  
184 presence of PM<sub>10</sub> (Fig. 4E). Similar results were obtained in NDV-infected A549 cells in presence  
185 of PM<sub>10</sub> (Supplementary Fig. S3B-E). Related results were obtained by re-analysing the GEO  
186 dataset GSE27973 of rhinovirus infection and CSE exposure in human bronchial epithelial cell  
187 lines (Supplementary Fig. S4A-B). Additionally, these metabolic pathways-related genes were  
188 found to be associated with many pathological states (Supplementary Fig. S4C). Overall our data  
189 concludes that upon PM<sub>10</sub> treatment during RNA virus infection, particularly, influenza virus  
190 infection, PM<sub>10</sub> significantly enhances the virus infection by down- regulating innate immune  
191 responses and upregulating different metabolic processes, that might cater air pollutant to enhance  
192 virus infectivity within the cells and manifold enhance respiratory damage.

193

#### 194 **Knockdown of metabolism-associated genes involved in virus replication**

195 To investigate the correlation between the upregulated metabolic pathways-related genes and their  
196 influence on virus infection upon PM<sub>10</sub> treatment, we selected CYP1A1, VIPR1 and PPP1R14A  
197 genes because these genes were significantly upregulated in our RNA sequencing analysis and  
198 were their role is poorly understood. The CYP1A1 involved in xenobiotic metabolic pathways,

199 which is one of the metabolic pathways aiding virus infections, VIPR1 is associated with G-protein  
200 coupled receptor pathway and PPP1R14A involved in vascular smooth muscle contraction and  
201 oxytocin pathway which were directly or indirectly related to virus infectivity within the host cell.  
202 To this end, we performed knockdown study of CYP1A1, VIPR1 and PPP1R14A in A549 cells.  
203 We used two different short hairpin (*sh*)-clones for each gene to knockdown the expression of  
204 CYP1A1, VIPR1 and PPP1R14A genes respectively as shown in the schematic workflow (Fig.  
205 5A-C). Particularly, knock down of these genes in presence of NDV infection in A549 cells, leads  
206 to significant suppression the virus infection, notably, the knockdown substantially reduced the  
207 gene expression (Fig. 5A-C) suggesting that upregulated metabolic pathways-related genes in  
208 presence of airborne particulate matter (PM<sub>10</sub>) support virus infections that further contribute to  
209 the severity of respiratory related diseases or highly pathogenic respiratory virus infections, like  
210 influenza.

211

212

213

214

215

216

217

218

219

220

221

## 222 **DISCUSSION**

223 In modern world, air pollution and emergence of novel microbial pathogens infecting through  
224 respiratory route has been included as the top threat to global health in the 13th General Programme  
225 of work, by WHO which aims to cover more than three billion people against the health  
226 emergencies from 2019-2023. ([https://www.who.int/about/what-we-do/thirteenth-general-](https://www.who.int/about/what-we-do/thirteenth-general-programme-of-work-2019-2023)  
227 [programme-of-work-2019-2023](https://www.who.int/about/what-we-do/thirteenth-general-programme-of-work-2019-2023)). Air pollution is a one of key risk factor for respiratory route or  
228 metabolism-associated diseases , and its adverse effects include morbidity and premature deaths  
229 throughout the world [45]. Particulate matter contributes to the majority of lethal effects caused  
230 by air pollution, which differs according to the geographical area. Particularly in India, where air  
231 pollution is predominant factor in major cities like, New Delhi, Bengaluru, Pune and so on. There  
232 were so far, very fewer studies which links particulate matter with the health and immunity in  
233 context to respiratory virus infections [37, 46]. Air pollutants are one of the major health concerns  
234 especially in inducing the adverse effects during pathogenic infections. Though these pollutants  
235 modulate the host defense and enhance susceptibility and severity during infection, the underline  
236 mechanisms are poorly understood [47]. Influenza is also included among the topmost threats by  
237 WHO and suggested to have pandemic potential. Influenza infection peaks during the winter  
238 season and cause frequent seasonal endemics, as well as sudden unforeseen pandemics. It spreads  
239 readily, and there is no proper vaccination available, therefore, it's been a major health as well as  
240 an economic burden throughout the world. The factors contributing to the emergence of a sudden  
241 pandemic strain of influenza is not well understood. Environmental factors play an essential role  
242 in the severity and spread of respiratory infections particularly influenza infection. Few studies  
243 explained the direct causative effects of ambient pollutants and other similar causative agents like  
244 cigarette smoke extracts, diesel exhaust on various lung infections and especially on the severity

245 of common cold occur by rhinovirus [37, 41, 48]. Different studies provide varied results over the  
246 impact of particulate matter in lung infections, as they are from different geographical origins [44,  
247 49, 50]. In a developing country like India, the level of ambient airborne particulate matter,  
248 especially PM<sub>10</sub>, increased in the past decade due to heavy industrialization. PM<sub>10</sub> isolation from  
249 Indian subcontinent and its deleterious effects on human health in context to hampering the innate  
250 immune defense, against RNA virus infections are not reported yet.

251 Herewith in this particular study, we sought to understand whether PM<sub>10</sub> exposure leads to  
252 significant modification of innate immune responses and viral infectivity in human lung epithelial  
253 cell lines, A549. Additionally, we focused to explore the overall cellular changes occur when cells  
254 were exposed to PM<sub>10</sub> and virus infection together. We also aimed to underpin the mechanism  
255 behind the intensification of influenza (H5N1) virus and other RNA virus infections like NDV in  
256 presence of airborne particulate matter (PM<sub>10</sub>). These cellular outcomes persuaded us to perform  
257 the RNA sequencing and analyse transcriptomic profile to unravelled the cellular changes during  
258 PM<sub>10</sub> exposure during infection.

259 We used PM<sub>10</sub> in our study obtained from Bengaluru city. Bengaluru is one of the heavily  
260 industrialized area in India. Therefore, studying the characteristics of ambient particulate matter  
261 around Bengaluru area is of importance. Initially, we characterized the PM<sub>10</sub> by performing SEM-  
262 EDS analysis, and reported the morphological features and chemical composition of the particulate  
263 matter as revealed by imaging analysis. PM<sub>10</sub> and its impact on airway was investigated by  
264 exposing the cells with PM<sub>10</sub> and infecting them with different RNA viruses like NDV and H5N1  
265 flu virus. Our results demonstrate the consequences of both air pollutant and virus infection.  
266 Interestingly, we observed that PM<sub>10</sub> isolated from the Bengaluru demonstrate that PM<sub>10</sub>  
267 suppresses innate immunity and significantly elevate viral replication. Previously, it has been

268 shown that antiviral response was suppressed upon CSE exposure during rhinovirus infection in  
269 human bronchial epithelial cell lines [41]. This prompted us to test the effect of PM<sub>10</sub> on the  
270 enhanced infectivity of highly pathogenic avian H5N1 influenza infection and decipher the  
271 molecular mechanism.

272 Although, few studies are reported the global transcriptomic changes, in presence PM<sub>10</sub> by  
273 microarray analysis. We, for the first time, used high throughput RNA sequencing to study the  
274 overall changes in the gene expression upon PM<sub>10</sub> exposure during the viral infection of highly  
275 pathogenic avian Influenza (HPAI) H5N1 virus in the lung carcinoma cells, A549. RNA  
276 sequencing analysis identified that majority of genes are significantly downregulated were  
277 involved in immune-related pathways, cytokine signalling, and few other inflammatory pathways.

278 In addition to this, we observed a significant increase in the expression of genes involved in various  
279 metabolic pathways, which were previously remain unknown, particularly in air pollution. We  
280 validated RNA sequencing results for four of the top hits genes namely VIPR1 (vasoactive  
281 intestinal peptide 1), CYP1A1 (cytochrome P450, family 1, subfamily A member1 also known  
282 as aryl hydrocarbon hydroxylase), ALDH1A3 (aldehyde dehydrogenase 1, family member 3A)  
283 and PPP1R14A (protein phosphatase 1 regulatory inhibitor subunit 14A) using quantitative qRT-  
284 PCR analysis. These selected genes are, VIPR1, mainly located on plasma membrane and  
285 PPP1R14A majorly located on nucleus and cytoskeleton were moderately found to be involved in  
286 virus infections like HIV-1 and influenza as reported by an *in-vitro* study and an *in-silico*  
287 phosphoproteomics study in human macrophages respectively [51-53]. CYP1A1 was recently  
288 reported to be involved in many virus infections especially hepatitis B and hepatitis C virus [54-  
289 56]. One such report superficially uncovers the induction of CYP1A1 in presences of PM<sub>10</sub> [57].  
290 Additionally, induction of CYP1A1 in presence of diesel exhaust particles were extensively

291 reported in human bronchial cells [58] . Apart from studies related to different types of cancers  
292 [59, 60] , ALDH1A3 was also previously reported in connection with virus infections like human  
293 papilloma virus and respiratory syncytial virus [61-63] . Altogether, these significant differentially  
294 expressed genes noted in our study related to different metabolic modifications inside the cell and  
295 reasonably linked to virus infections, therefore, we selected these genes for validation in context  
296 to RNA virus infectivity. We demonstrated by *sh*-RNA mediated transient silencing that these  
297 genes significantly reduced the viral replication. This states the importance of these metabolic  
298 pathway-related genes in regulation of pathogenic burden during viral infection.

299 Overall, this study highlights the effect of PM<sub>10</sub> exposure upon virus infection that affects the lung  
300 airways to cause severe respiratory damage. And high throughput RNA sequencing was performed  
301 for the first time, in context to Indian subcontinent distribution of particulate matter (PM<sub>10</sub>). PM<sub>10</sub>  
302 collected and isolated to study the transcriptomic changes upon its exposure during influenza  
303 infection in A549 cell lines. The overall summary of the study was graphically illustrated in Figure  
304 5D-E. There were very few studies that reported the link between PM<sub>10</sub> exposure and enhanced  
305 viral infections [64, 65] . Our study not only reported the status of viral replication upon PM<sub>10</sub>  
306 exposure, but also examined the role of metabolic pathways - associated genes involved in the  
307 viral replication. Still, this study requires further *in-vivo* analysis using mice models in order to  
308 explore the effect of pollutant under physiological condition after PM<sub>10</sub> exposure. Further studies  
309 were needed to uncover the connecting links between other respiratory infectious diseases and the  
310 use of PM<sub>10</sub> from different geographical locations, seasonal variation, which will give better  
311 insights about the effects of PM<sub>10</sub> over various lung infections including influenza virus infection.

312

313

## 314 **MATERIALS AND METHODS**

### 315 **Cell lines and reagents**

316 A549 human alveolar basal epithelial cells (Cell Repository, NCCS, India) were cultured in  
317 Dulbecco's modified Eagle's medium (DMEM) supplemented with 10% fetal bovine serum (FBS)  
318 and 1% Antibiotic-Antimycotic solution. DMEM, FBS and Antibiotic-Antimycotic solution were  
319 purchased from Invitrogen. Ambient particulate matter of coarse particle size PM<sub>10</sub> was obtained  
320 from Dr. Gangamma S. which was collected and isolated in appropriate solvent media from the  
321 geographical regions of Bengaluru city, at NITK, Surathkal, Mangaluru, Karnataka. A549 cells  
322 were seeded in 12 well culture plate at a concentration of 3x10<sup>5</sup>/well overnight (37°C, 5% CO<sub>2</sub>).  
323 Cells were treated with PM<sub>10</sub> along with controls namely blank and/or LPS (100 ng) for 24 hours  
324 prior to infection. Plasmids containing Firefly Luciferase gene under *IFNβ* and *ISRE* promoters,  
325 were obtained from Professor Shizuo Akira's (Osaka University, Japan). All sh- clones, were  
326 obtained from the whole RNAi human library for shRNA mediating silencing (Sigma, Aldrich)  
327 maintained at IISER, Bhopal, India.

### 328 **Virus Infection**

329 Airborne particulate matter (PM<sub>10</sub>) treated A549 cells were infected with new-castle disease virus  
330 (NDV), highly pathogenic avian influenza virus (H5N1) and vaccine strain PR-8 virus (H1N1) at  
331 respective multiplicity of infection as mentioned in the figures and/or figure legends. PM<sub>10</sub> treated  
332 A549 cells were washed by 1X PBS (phosphate-buffered saline) solution and infected with  
333 appropriate RNA viruses in serum-free media as per the subsequent experiment then after 60  
334 minutes, virus containing media was removed from the cells and cells were washed once with 1X  
335 PBS solution. Then cells were again supplemented with new PM<sub>10</sub> containing DMEM media for  
336 24 hours. Samples were then harvested and forwarded for respective quantitative analysis.



### 337 **Sampling of airborne particulate matter**

338 Bangalore is an inland city (12°58' N, 77°34') situated on the south-central part of India at a height  
339 over 900m above sea level. General sources of airborne particulate matter (PM) in the city include  
340 vehicular emissions, industrial emissions and re-suspended road dust  
341 ([http://www.cpcbenvi.nic.in/envi\\_newsletter/Air%20Quality%20of%20Delhi.pdf](http://www.cpcbenvi.nic.in/envi_newsletter/Air%20Quality%20of%20Delhi.pdf);  
342 [https://www.teriin.org/sites/default/files/2018-08/Report\\_SA\\_AQM-Delhi-NCR\\_0.pdf](https://www.teriin.org/sites/default/files/2018-08/Report_SA_AQM-Delhi-NCR_0.pdf);  
343 <http://164.100.107.13/Bangalore.pdf>). Air samples were collected from six ambient air quality  
344 monitoring sites of Karnataka State Pollution Control Board (KSPCB). Particulate matter with  
345 aerodynamic diameter less than 10µm was collected using high volume samplers (Poll tech, India).  
346 The samples were collected on quartz fiber filter paper (GE healthcare, India). The filter papers  
347 were de-pyrogenated and conditioned prior to sampling [66]. To ensure contamination free  
348 sampling, field blanks were included in the samples. After sampling, filter papers were sealed in  
349 de-pyrogenated aluminium foil and transported to the laboratory. The samples were stored at -  
350 20°C until further processing. PM on the filter was extracted into methanol. Further, methanol was  
351 purged and samples were reconstituted with DMSO [67, 68] . Samples were pooled and used for  
352 further experiments.

353

### 354 **Particulate Matter (PM<sub>10</sub>) dose standardization**

355 For all the preliminary experiments three different dosage form of PM<sub>10</sub> was used in the ratios 1:1  
356 (PM<sub>10</sub>: DMEM), 0.2:1 (PM<sub>10</sub>: DMEM) and 0.5:1 (PM<sub>10</sub>: DMEM) named as PM(I), PM(II) and  
357 PM(III) respectively. And after the standardization through different experiments PM(I) that is 1:1  
358 (PM<sub>10</sub>: DMEM) dosage of PM<sub>10</sub> was used for subsequent experiments.

359

### 360 **SEM-EDS Analysis**

361 Particulate Matter (PM) dissolved in appropriate solvents was installed on the metallic stabs in the  
362 form of droplets and dried overnight in the desiccator for complete solvent dry process. Samples  
363 were then loaded on the high-resolution field emission scanning electron microscope (SEM) (HR  
364 FESEM) from Zeiss, model name ULTRA Plus at IISER Bhopal for PM<sub>10</sub> morphological analysis.  
365 Then chemical composition of the PM<sub>10</sub> was elucidated by the Energy Dispersive X-ray  
366 spectrometer (EDS) component of the scanning electron microscope.

### 367 **Quantitative real-time reverse transcription PCR**

368 Total RNA was extracted with the Trizol reagent (Ambion/Invitrogen) and used to synthesize  
369 cDNA with the iScript cDNA Synthesis Kit (BioRad, Hercules, CA, USA) according to the  
370 manufacturer's protocol. Gene expression was measured by quantitative real-time PCR using  
371 gene-specific primers and SYBR Green (Biorad, Hercules, CA, USA). The 18S gene was used as  
372 a reference control. Real time quantification was done using StepOne Plus Real time PCR Systems  
373 by Applied BioSystems (Foster City, CA, USA).

### 374 **Luciferase Reporter assays**

375 A549 cells ( $5 \times 10^4$ ) were seeded into a 12-well plate and transiently transfected with 50 ng of the  
376 transfection control pRL-TK plasmid (*Renilla* luciferase containing plasmid) and 200 ng of the  
377 luciferase reporter plasmid (*Firefly* luciferase containing plasmid) of IFN $\beta$  and ISRE promoters.  
378 After 12 hours cells were treated with PM<sub>10</sub> in the ratio 1:1 (PM<sub>10</sub>: DMEM) and Blank as a control  
379 for 24 hours. Then after cells were infected with NDV (MOI 2) for 24 hours. The cells were lysed  
380 at 24 hours after final infection, and finally the luciferase activity in total cell lysates was measured  
381 with Glomax (Promega, Madison, WI, USA).

382

383 **Enzyme-linked immunosorbent assay (ELISA)**

384 A549 cells were treated with PM<sub>10</sub> in the ratio 1:1 (PM<sub>10</sub>: DMEM) and Blank as a control after 24  
385 hours of seeding. The culture media were harvested at 36 hours after particulate matter treatment  
386 and were analysed by specific ELISA kits (Becton Dickinson) according to the manufacturer's  
387 instructions to determine the amounts of *IL6* that were secreted by the cells.

388 **Cell count Trypan Blue assay**

389 A549 cells were seeded and after 24 hours treated with PM<sub>10</sub> and blank for 24 hours before NDV  
390 infection. Cell supernatant were collected after 36 hours of infection, mixed with trypan blue dye  
391 (Sigma) in the ratio 1:1. The mixture then used for counting the dead cells under the microscope.

392 **Microscopy**

393 A549 cells were seeded along with cover slips in low confluency and next day treated with PM<sub>10</sub>  
394 at a dosage of 1:1 [PM: DMEM] for 24 hours prior to virus infection. Cells were then infected with  
395 NDV-GFP (3 MOI) in serum free media for 1 hour. After infection cells were again supplemented  
396 with complete media and treated with PM<sub>10</sub> at a dosage of 1:1 (PM<sub>10</sub>: DMEM) for 24 hours at 37°C,  
397 5% CO<sub>2</sub>. Cells were then washed twice with PBS for 5 minutes and fixed in 4% PFA for 20 minutes  
398 again washed in PBS and incubated with DAPI (20 mg/ml) for 30 minutes at room temperature  
399 and finally washed thrice with PBS. Cover slips then containing cells were carefully mounted on  
400 to the glass slides using Fluoroshield (Sigma) as mounting media. Slide was then kept for few  
401 hours for drying before imaging. Images were visualized at 40X with Apotome – AXIO  
402 fluorescence microscope by Zeiss.

403 **NGS Analysis**

404 Total RNA was extracted using TRIzol reagent (Ambion/Invitrogen) and assessed for quality. The  
405 RNA-Seq paired end libraries were prepared from the QC passed RNA samples using Illumina

406 TrueSeq stranded mRNA sample prep kit. Libraries were sequenced using NextSeq500 with a read  
407 length (2x75bp), by Eurofins Genomic India Private Limited, India. The Raw reads were assessed  
408 for quality using FastQC (Andrews S et al, 2010). The filtering of reads and the removal of  
409 adapters were performed using the tool Trimmomatic [69]. Approximately 18 million base pair  
410 reads were mapped to the human transcriptome (hg38), using Kallisto [70] and the abundance of  
411 the assembled coding transcriptome were projected as transcripts per million (TPM). The  
412 transcripts level abundance counts were converted into gene-level abundance counts using the R  
413 package, Tximport [71] . Differential expression analysis was performed using Limma package  
414 [72]. The genes which were differentially expressed ( $-1.5 < \text{Log FC} < 1.5$ ) were selected and the  
415 gene ontology analysis were performed using DAVID tool [73] . Bubble plots, circle plot, chord  
416 plots were generated from the gene ontology and pathway enrichment results generated by DAVID  
417 tool, using the R package GOplot [74].

#### 418 **Statistical analysis**

419 All experiments were carried out along with the appropriate controls, indicated as  
420 untreated/untransfected cells (Ctrl) or transfected with the transfection reagent alone (Mock).  
421 Experiments were performed in duplicates or triplicates for at least two or three times  
422 independently. GraphPad Prism 5.0 (GraphPad Software, La Jolla, CA, USA) was used for  
423 statistical analysis. The differences between two groups were compared by using an unpaired two-  
424 tailed Student's t-test. While the differences between three groups or more were compared by  
425 using analysis of variance (ANOVA) with Tukey test. Differences were considered to be  
426 statistically significant when  $P < 0.05$ . Statistical significance in the figures is indicated as follows:  
427 \*\*\* $P < 0.001$ , \*\* $P < 0.01$ , \* $P < 0.05$ ; *ns*, not significant.

428 **Acknowledgments:** We greatly acknowledge Dr. Gangamma S. for providing particulate matter  
429 (PM<sub>10</sub>) in its isolated form collected from the city of Bengaluru. We thank Director, ICAR-  
430 NIHSAD for providing BSL-3 facility to conduct H5N1 experiments. We express our humble  
431 gratitude towards Dr. Santhalembi Chingtham – for infecting the cells with Influenza (H5N1) virus  
432 in BSL-3 core facility at ICAR - NIHSAD Laboratory. We are grateful to Indian Institute of  
433 Science Education and Research (IISER) Bhopal for providing the Central Instrumentation  
434 Facility. We thank all the members of the laboratory of immunology and infectious disease biology  
435 for helpful discussions. We acknowledge shutterstock.com for an image.

436

437 **Funding:** This work was supported by SERB-DST grant (DST No. SB/S3/CEE/030/2014) to H.K.  
438 as principal investigator of the project and G.S. as Co-PI of the project. R.M. is supported by the  
439 IISER Bhopal institutional fellowship.

440

441 **Conflict of interests:** The authors declare no conflict of interests.

442

443 **Data and materials availability:** The NGS (RNA-Sequencing) data for expression profiling  
444 reported in this paper have been deposited in the GenBank database (accession no. yet to receive  
445 from NCBI).

446 **REFERENCES:**

- 447 1. Cohen, A.J., et al., *Estimates and 25-year trends of the global burden of disease*  
448 *attributable to ambient air pollution: an analysis of data from the Global Burden of*  
449 *Diseases Study 2015*. Lancet, 2017. **389**(10082): p. 1907-1918.
- 450 2. Katsouyanni, K., et al., *Air pollution and health: a European and North American*  
451 *approach (APHENA)*. Res Rep Health Eff Inst, 2009(142): p. 5-90.
- 452 3. Lelieveld, J., et al., *The contribution of outdoor air pollution sources to premature*  
453 *mortality on a global scale*. Nature, 2015. **525**(7569): p. 367-71.
- 454 4. Liu, C., et al., *Ambient Particulate Air Pollution and Daily Mortality in 652 Cities*. N Engl  
455 J Med, 2019. **381**(8): p. 705-715.
- 456 5. Romieu, I., et al., *Multicity study of air pollution and mortality in Latin America (the*  
457 *ESCALA study)*. Res Rep Health Eff Inst, 2012(171): p. 5-86.
- 458 6. Wong, C.M., et al., *Public Health and Air Pollution in Asia (PAPA): a multicity study of*  
459 *short-term effects of air pollution on mortality*. Environ Health Perspect, 2008. **116**(9): p.  
460 1195-202.
- 461 7. Deng, Q., et al., *Particle deposition in the human lung: Health implications of particulate*  
462 *matter from different sources*. Environ Res, 2019. **169**: p. 237-245.
- 463 8. Dai, L., et al., *Associations of fine particulate matter species with mortality in the United*  
464 *States: a multicity time-series analysis*. Environ Health Perspect, 2014. **122**(8): p. 837-42.
- 465 9. Samet, J.M., et al., *Fine particulate air pollution and mortality in 20 U.S. cities, 1987-*  
466 *1994*. N Engl J Med, 2000. **343**(24): p. 1742-9.
- 467 10. Chen, R., et al., *Fine Particulate Air Pollution and Daily Mortality. A Nationwide Analysis*  
468 *in 272 Chinese Cities*. Am J Respir Crit Care Med, 2017. **196**(1): p. 73-81.
- 469 11. Lu, F., et al., *Systematic review and meta-analysis of the adverse health effects of ambient*  
470 *PM2.5 and PM10 pollution in the Chinese population*. Environ Res, 2015. **136**: p. 196-  
471 204.
- 472 12. India State-Level Disease Burden Initiative Air Pollution, C., *The impact of air pollution*  
473 *on deaths, disease burden, and life expectancy across the states of India: the Global*  
474 *Burden of Disease Study 2017*. Lancet Planet Health, 2019. **3**(1): p. e26-e39.
- 475 13. Harrison, R.M. and J. Yin, *Particulate matter in the atmosphere: which particle properties*  
476 *are important for its effects on health?* Sci Total Environ, 2000. **249**(1-3): p. 85-101.
- 477 14. Manojkumar, N. and B. Srimuruganandam, *Health effects of particulate matter in major*  
478 *Indian cities*. Int J Environ Health Res, 2019: p. 1-13.
- 479 15. Jain, V., S. Dey, and S. Chowdhury, *Ambient PM2.5 exposure and premature mortality*  
480 *burden in the holy city Varanasi, India*. Environ Pollut, 2017. **226**: p. 182-189.
- 481 16. Sharma, A.K., P. Baliyan, and P. Kumar, *Air pollution and public health: the challenges*  
482 *for Delhi, India*. Rev Environ Health, 2018. **33**(1): p. 77-86.
- 483 17. Sharma, M., et al., *Effects of particulate air pollution on the respiratory health of subjects*  
484 *who live in three areas in Kanpur, India*. Arch Environ Health, 2004. **59**(7): p. 348-58.
- 485 18. Sharma, S., et al., *Indoor air quality and acute lower respiratory infection in Indian urban*  
486 *slums*. Environ Health Perspect, 1998. **106**(5): p. 291-7.
- 487 19. Khafaie, M.A., et al., *Air pollution and respiratory health among diabetic and non-diabetic*  
488 *subjects in Pune, India-results from the Wellcome Trust Genetic Study*. Environ Sci Pollut  
489 Res Int, 2017. **24**(18): p. 15538-15546.

- 490 20. Janssen, N.A., et al., *Short-term effects of PM<sub>2.5</sub>, PM<sub>10</sub> and PM<sub>2.5-10</sub> on daily mortality*  
491 *in The Netherlands*. Sci Total Environ, 2013. **463-464**: p. 20-6.
- 492 21. Carugno, M., et al., *Air pollution exposure, cause-specific deaths and hospitalizations in a*  
493 *highly polluted Italian region*. Environ Res, 2016. **147**: p. 415-24.
- 494 22. Lin, M., D.M. Stieb, and Y. Chen, *Coarse particulate matter and hospitalization for*  
495 *respiratory infections in children younger than 15 years in Toronto: a case-crossover*  
496 *analysis*. Pediatrics, 2005. **116**(2): p. e235-40.
- 497 23. Donaldson, K., M.I. Gilmour, and W. MacNee, *Asthma and PM<sub>10</sub>*. Respir Res, 2000. **1**(1):  
498 p. 12-5.
- 499 24. Consonni, D., et al., *Outdoor particulate matter (PM<sub>10</sub>) exposure and lung cancer risk in*  
500 *the EAGLE study*. PLoS One, 2018. **13**(9): p. e0203539.
- 501 25. Hamra, G.B., et al., *Outdoor particulate matter exposure and lung cancer: a systematic*  
502 *review and meta-analysis*. Environ Health Perspect, 2014. **122**(9): p. 906-11.
- 503 26. Li, Y.G. and X. Gao, *Epidemiologic studies of particulate matter and lung cancer*. Chin J  
504 Cancer, 2014. **33**(8): p. 376-80.
- 505 27. Chu, Y.H., et al., *Association between fine particulate matter and oral cancer among*  
506 *Taiwanese men*. J Investig Med, 2019. **67**(1): p. 34-38.
- 507 28. Rivas-Santiago, C.E., et al., *Air pollution particulate matter alters antimycobacterial*  
508 *respiratory epithelium innate immunity*. Infect Immun, 2015. **83**(6): p. 2507-17.
- 509 29. Sarkar, S., et al., *Season and size of urban particulate matter differentially affect*  
510 *cytotoxicity and human immune responses to Mycobacterium tuberculosis*. PLoS One,  
511 2019. **14**(7): p. e0219122.
- 512 30. Hirota, J.A., et al., *The nucleotide-binding domain, leucine-rich repeat protein 3*  
513 *inflammasome/IL-1 receptor I axis mediates innate, but not adaptive, immune responses*  
514 *after exposure to particulate matter under 10 µm*. Am J Respir Cell Mol Biol, 2015.  
515 **52**(1): p. 96-105.
- 516 31. Overocker, J. and J.C. Pfau, *Cytokine Production Modified by System X(c)- After PM<sub>10</sub>*  
517 *and Asbestos Exposure*. J Young Investig, 2012. **23**(6): p. 34-39.
- 518 32. Tang, Q., et al., *Fine particulate matter from pig house induced immune response by*  
519 *activating TLR4/MAPK/NF-κB pathway and NLRP3 inflammasome in alveolar*  
520 *macrophages*. Chemosphere, 2019. **236**: p. 124373.
- 521 33. Bengalli, R., et al., *Release of IL-1 beta triggered by Milan summer PM<sub>10</sub>: molecular*  
522 *pathways involved in the cytokine release*. Biomed Res Int, 2013. **2013**: p. 158093.
- 523 34. Ling, S.H. and S.F. van Eeden, *Particulate matter air pollution exposure: role in the*  
524 *development and exacerbation of chronic obstructive pulmonary disease*. Int J Chron  
525 Obstruct Pulmon Dis, 2009. **4**: p. 233-43.
- 526 35. Ni, L., C.C. Chuang, and L. Zuo, *Fine particulate matter in acute exacerbation of COPD*.  
527 Front Physiol, 2015. **6**: p. 294.
- 528 36. Wen, C.P. and W. Gao, *PM<sub>2.5</sub>: an important cause for chronic obstructive pulmonary*  
529 *disease?* Lancet Planet Health, 2018. **2**(3): p. e105-e106.
- 530 37. MacNee, W. and K. Donaldson, *Mechanism of lung injury caused by PM<sub>10</sub> and ultrafine*  
531 *particles with special reference to COPD*. Eur Respir J Suppl, 2003. **40**: p. 47s-51s.
- 532 38. Karr, C.J., et al., *Infant exposure to fine particulate matter and traffic and risk of*  
533 *hospitalization for RSV bronchiolitis in a region with lower ambient air pollution*. Environ  
534 Res, 2009. **109**(3): p. 321-7.



- 535 39. Vandini, S., et al., *Respiratory syncytial virus infection in infants and correlation with*  
536 *meteorological factors and air pollutants*. Ital J Pediatr, 2013. **39**(1): p. 1.
- 537 40. Kaan, P.M. and R.G. Hegele, *Interaction between respiratory syncytial virus and*  
538 *particulate matter in guinea pig alveolar macrophages*. Am J Respir Cell Mol Biol, 2003.  
539 **28**(6): p. 697-704.
- 540 41. Proud, D., et al., *Cigarette smoke modulates expression of human rhinovirus-induced*  
541 *airway epithelial host defense genes*. PLoS One, 2012. **7**(7): p. e40762.
- 542 42. Xu, Z., et al., *Air pollution, temperature and pediatric influenza in Brisbane, Australia*.  
543 Environ Int, 2013. **59**: p. 384-8.
- 544 43. Clifford, H.D., K.L. Perks, and G.R. Zosky, *Geogenic PM(1)(0) exposure exacerbates*  
545 *responses to influenza infection*. Sci Total Environ, 2015. **533**: p. 275-82.
- 546 44. Huang, L., et al., *Acute effects of air pollution on influenza-like illness in Nanjing, China:*  
547 *A population-based study*. Chemosphere, 2016. **147**: p. 180-7.
- 548 45. Landrigan, P.J., *Air pollution and health*. Lancet Public Health, 2017. **2**(1): p. e4-e5.
- 549 46. Khilnani, G.C. and P. Tiwari, *Air pollution in India and related adverse respiratory health*  
550 *effects: past, present, and future directions*. Curr Opin Pulm Med, 2018. **24**(2): p. 108-116.
- 551 47. Becker, S. and J.M. Soukup, *Exposure to urban air particulates alters the macrophage-*  
552 *mediated inflammatory response to respiratory viral infection*. J Toxicol Environ Health  
553 A, 1999. **57**(7): p. 445-57.
- 554 48. Paulin, L. and N. Hansel, *Particulate air pollution and impaired lung function*. F1000Res,  
555 2016. **5**.
- 556 49. Feng, C., et al., *Impact of ambient fine particulate matter (PM2.5) exposure on the risk of*  
557 *influenza-like-illness: a time-series analysis in Beijing, China*. Environ Health, 2016. **15**:  
558 p. 17.
- 559 50. Liu, X.X., et al., *Effects of air pollutants on occurrences of influenza-like illness and*  
560 *laboratory-confirmed influenza in Hefei, China*. Int J Biometeorol, 2019. **63**(1): p. 51-60.
- 561 51. Temerozo, J.R., et al., *The Neuropeptides Vasoactive Intestinal Peptide and Pituitary*  
562 *Adenylate Cyclase-Activating Polypeptide Control HIV-1 Infection in Macrophages*  
563 *Through Activation of Protein Kinases A and C*. Front Immunol, 2018. **9**: p. 1336.
- 564 52. Bokaei, P.B., et al., *Identification and characterization of five-transmembrane isoforms of*  
565 *human vasoactive intestinal peptide and pituitary adenylate cyclase-activating polypeptide*  
566 *receptors*. Genomics, 2006. **88**(6): p. 791-800.
- 567 53. Soderholm, S., et al., *Phosphoproteomics to Characterize Host Response During Influenza*  
568 *A Virus Infection of Human Macrophages*. Mol Cell Proteomics, 2016. **15**(10): p. 3203-  
569 3219.
- 570 54. Ohashi, H., et al., *The aryl hydrocarbon receptor-cytochrome P450 1A1 pathway controls*  
571 *lipid accumulation and enhances the permissiveness for hepatitis C virus assembly*. J Biol  
572 Chem, 2018. **293**(51): p. 19559-19571.
- 573 55. Fattahi, S., et al., *Cytochrome P450 Genes (CYP2E1 and CYP1A1) Variants and*  
574 *Susceptibility to Chronic Hepatitis B Virus Infection*. Indian J Clin Biochem, 2018. **33**(4):  
575 p. 467-472.
- 576 56. Stavropoulou, E., G.G. Pircalabioru, and E. Bezirtzoglou, *The Role of Cytochromes P450*  
577 *in Infection*. Front Immunol, 2018. **9**: p. 89.
- 578 57. Kim, H.J., et al., *CYP1A1 gene polymorphisms modify the association between PM10*  
579 *exposure and lung function*. Chemosphere, 2018. **203**: p. 353-359.



- 580 58. Totlandsdal, A.I., et al., *Diesel exhaust particles induce CYP1A1 and pro-inflammatory*  
581 *responses via differential pathways in human bronchial epithelial cells.* Part Fibre Toxicol,  
582 2010. **7**: p. 41.
- 583 59. Croker, A.K., et al., *Differential Functional Roles of ALDH1A1 and ALDH1A3 in*  
584 *Mediating Metastatic Behavior and Therapy Resistance of Human Breast Cancer Cells.*  
585 Int J Mol Sci, 2017. **18**(10).
- 586 60. Flahaut, M., et al., *Aldehyde dehydrogenase activity plays a Key role in the aggressive*  
587 *phenotype of neuroblastoma.* BMC Cancer, 2016. **16**(1): p. 781.
- 588 61. Diamond, D.L., et al., *Proteome and computational analyses reveal new insights into the*  
589 *mechanisms of hepatitis C virus-mediated liver disease posttransplantation.* Hepatology,  
590 2012. **56**(1): p. 28-38.
- 591 62. Tulake, W., et al., *Upregulation of stem cell markers ALDH1A1 and OCT4 as potential*  
592 *biomarkers for the early detection of cervical carcinoma.* Oncol Lett, 2018. **16**(5): p. 5525-  
593 5534.
- 594 63. Puttini, S., et al., *ALDH1A3 Is the Key Isoform That Contributes to Aldehyde*  
595 *Dehydrogenase Activity and Affects in Vitro Proliferation in Cardiac Atrial Appendage*  
596 *Progenitor Cells.* Front Cardiovasc Med, 2018. **5**: p. 90.
- 597 64. Hirota, J.A., et al., *Urban particulate matter increases human airway epithelial cell IL-*  
598 *Ibeta secretion following scratch wounding and H1N1 influenza A exposure in vitro.* Exp  
599 Lung Res, 2015. **41**(6): p. 353-62.
- 600 65. Wang, J., et al., *Cigarette smoke inhibits BAFF expression and mucosal immunoglobulin*  
601 *A responses in the lung during influenza virus infection.* Respir Res, 2015. **16**: p. 37.
- 602 66. Gangamma, S., R.S. Patil, and S. Mukherji, *Characterization and proinflammatory*  
603 *response of airborne biological particles from wastewater treatment plants.* Environ Sci  
604 Technol, 2011. **45**(8): p. 3282-7.
- 605 67. Totlandsdal, A.I., et al., *The occurrence of polycyclic aromatic hydrocarbons and their*  
606 *derivatives and the proinflammatory potential of fractionated extracts of diesel exhaust*  
607 *and wood smoke particles.* J Environ Sci Health A Tox Hazard Subst Environ Eng, 2014.  
608 **49**(4): p. 383-96.
- 609 68. Bach, N., et al., *Cytokine responses induced by diesel exhaust particles are suppressed by*  
610 *PAR-2 silencing and antioxidant treatment, and driven by polar and non-polar soluble*  
611 *constituents.* Toxicol Lett, 2015. **238**(2): p. 72-82.
- 612 69. Bolger, A.M., M. Lohse, and B. Usadel, *Trimmomatic: a flexible trimmer for Illumina*  
613 *sequence data.* Bioinformatics, 2014. **30**(15): p. 2114-20.
- 614 70. Bray, N.L., et al., *Near-optimal probabilistic RNA-seq quantification.* Nat Biotechnol,  
615 2016. **34**(5): p. 525-7.
- 616 71. Sonesson, C., M.I. Love, and M.D. Robinson, *Differential analyses for RNA-seq: transcript-*  
617 *level estimates improve gene-level inferences.* F1000Res, 2015. **4**: p. 1521.
- 618 72. Ritchie, M.E., et al., *limma powers differential expression analyses for RNA-sequencing*  
619 *and microarray studies.* Nucleic Acids Res, 2015. **43**(7): p. e47.
- 620 73. Huang, D.W., et al., *The DAVID Gene Functional Classification Tool: a novel biological*  
621 *module-centric algorithm to functionally analyze large gene lists.* Genome Biol, 2007.  
622 **8**(9): p. R183.
- 623 74. Walter, W., F. Sanchez-Cabo, and M. Ricote, *GOplot: an R package for visually combining*  
624 *expression data with functional analysis.* Bioinformatics, 2015. **31**(17): p. 2912-4.
- 625

626 **Figure Legends:**

627 **Figure 1: Morphological features of PM<sub>10</sub>** - Scanning electron images of coarse airborne particulate matter PM<sub>10</sub>.

628 (A) Image of blank solution with alone with no PM dissolved in it. (B-T) Images of different shapes with varied  
629 structures representing the different characteristic morphological features of PM in the samples.

630 **Figure 2: PM<sub>10</sub> regulates the innate immune response upon RNA virus infection** – Quantification of innate

631 immune response. A549 cells were treated with PM<sub>10</sub> and control mentioned as blank for (A) 24 hours then harvested

632 in Trizol to quantify the mRNA expression of *IFNβ* and *IL6* by qRT-PCR. (B) 36 hours then cell supernatant was

633 collected to measure the protein level of *IL6* by ELISA. (C) Schematic representation of workflow for quantification

634 of *IFNβ* and ISRE promoter activities by luciferase assay as indicated in A549 cells. NDV represents new-castle

635 disease virus infection at MOI = 2. (D) Schematic work flow of PM<sub>10</sub> exposure and NDV infection. (E) Quantification

636 of *IFNβ* and *IL6* mRNA transcripts in uninfected (control), mock infected, blank treated and PM<sub>10</sub> exposed cells by

637 qRT-PCR. (G) Schematic work flow of PM<sub>10</sub> exposure and H5N1 influenza infection. (H) Quantification of *IFNβ*

638 and *IL6* mRNA transcripts in uninfected (control), mock infected, blank treated and PM<sub>10</sub> exposed cells by qRT-PCR.

639 Data are mean +/- SEM of triplicate samples from single experiment and are representative of two independent

640 experiments. \*\*\**P*<0.001, \*\**P*<0.01 and \**P*<0.05 by one-way ANOVA Tukey test and unpaired t-test.

641 **Figure 3: PM<sub>10</sub> elevates the RNA virus infection** – (A-F) Estimation of viral replication in A549 cells exposed with

642 PM<sub>10</sub> for 24 hours before virus infection at MOI = 2. (A) Schematic work flow of the experiment, PM<sub>10</sub> enhances the

643 NDV abundance (viral transcripts) in the cells compared to control groups (uninfected control, mock infected, blank

644 treated and PM<sub>10</sub> exposed). (B-C) Schematic work flow of the experiment, PM<sub>10</sub> enhances the H5N1 and H1N1

645 abundance (viral transcripts) in the cells compared to control groups (uninfected control, mock infected, blank treated

646 and PM<sub>10</sub> exposed). (D) Schematic work flow for microscopy: A549 cells were exposed with PM<sub>10</sub> then after infected

647 with GFP – labelled NDV for 24 hours, cells in the cover slips were then fixed as per the protocol described in methods

648 section and estimated for GFP positive signals quantified as (E) total number of NDV-GFP infected cells and (F)

649 intensity of GFP signals in infected cells. (G) Schematic work flow to estimate the cell death in cell supernatant after

650 PM<sub>10</sub> exposure and NDV infection in A549 cells. Cells (dead) were counted by the trypan blue counting assay. Data

651 are mean +/- SEM of triplicate samples from single experiment and are representative of two independent experiments.

652 \*\*\**P*<0.001 by one-way ANOVA Tukey test and unpaired t-test.

653

654 **Figure 4: Transcriptomic analysis shows PM<sub>10</sub> enhances abundance of metabolic pathways-related transcripts**

655 **(genes) during H5N1 infection** - (A) Schematic outline of PM<sub>10</sub> exposure and H5N1 infection (MOI 2) in A549 cells

656 at indicated time. Cells were subjected to whole transcriptome sequencing and differential gene expression analysis.

657 (B) Volcano plot represents differential expression of genes between two groups of samples (mock H5N1 infected

658 and PM<sub>10</sub> exposed plus H5N1 infected) during H5N1 infection in A549 cells. For each gene: *P-value* is plotted against

659 fold change (mock vs PM<sub>10</sub>). Significantly differentially expressed genes are marked in red colour while genes which

660 are altered (>1.5-fold) are marked in blue colour. (C) Gene Ontology analysis performed as per the protocol mentioned

661 in methods section represents the top differentially expressed genes in ontology terms: BP (biological processes), CC

662 (cellular components) and MF (molecular functions) respectively depicted by bubble plot and circle plot generated

663 through R package GOplot. (D) Pathway enrichment analysis performed as per the protocol mentioned in methods

664 section. Chord plot represents the differentially expressed genes and their connection with the top enriched pathways.

665 Circle plot represents the top enriched pathways and status of the genes contributing to the pathways by their logFC

666 and Z-score. (E-H) Quantification (measured by qRT-PCR) and validation of the fold changes in the abundances of

667 significantly expressed metabolic pathways related transcripts: VIPR1, CYP1A1, ALDH1A3 and PPP1R14A in the

668 samples of A549 cells; untreated (control), mock H5N1 infected (H5N1) and PM<sub>10</sub> exposed plus H5N1 infected

669 (H5N1+PM), analyzed by RNA- Sequencing. For figure (E-H): Data are mean +/- SEM of triplicate samples from

670 single experiment and are representative of two independent experiments. \*\*\**P*<0.001 and \*\**P*<0.01 by one-way

671 ANOVA Tukey test and unpaired t-test.

672 **Figure 5: Knockdown of validated genes reduces RNA virus infection** – A549 cells were transiently transfected

673 with 1.5µg of two respective *sh*-clones of each indicated genes or scrambled control for 72 hours then infected with

674 NDV (MOI 2) for 24 hours and subjected to the quantification of the NDV viral RNA transcripts and the respective

675 indicated transcripts or genes (A) CYP1A1, (B) VIPR1 and (C) PPP1R14A. (D) Graphical representation of the study:

676 CYP1A1, PPP1R14A and VIPR1 at their respective location (endoplasmic reticulum, cytoskeleton-nucleus and

677 plasma membrane respectively) within the cell induced upon RNA virus infection and PM<sub>10</sub> exposure to increase viral

678 infection in presence of airborne PM<sub>10</sub>. PRRs – Pattern Recognition Receptors to sense the viral particles. Overall

679 immune responses were downregulated in PM<sub>10</sub> treated cells. (E) Cumulative effect of PM<sub>10</sub> and virus infection

680 enhance respiratory damage and overall virus infection in lungs at the organismic level.

681

682 **Supplementary Figure Legends**

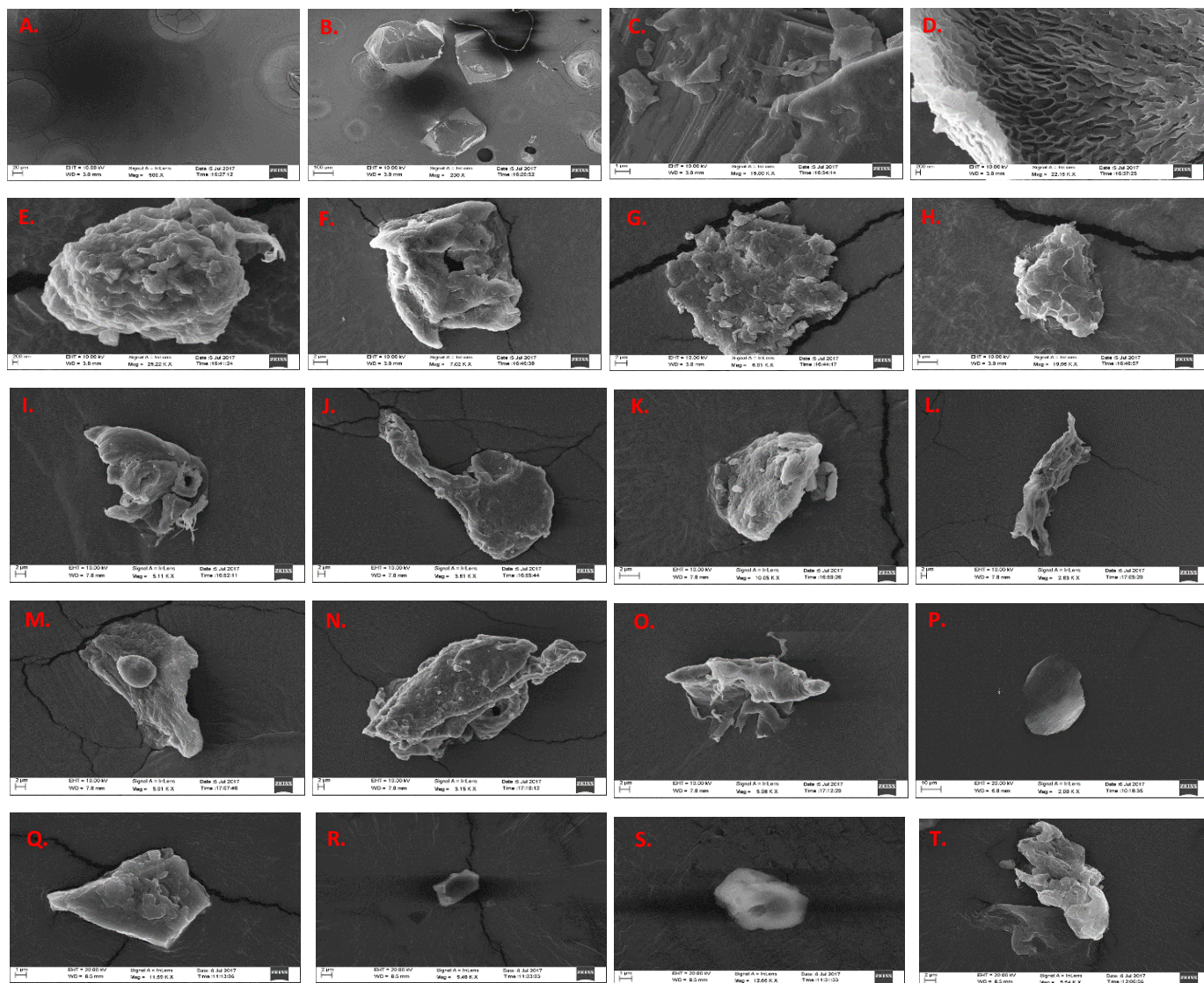
683 **Supplementary Figure 1: SEM-EDS analysis of PM<sub>10</sub>.** Scanning electron images and energy – dispersive X-ray  
684 spectra of coarse airborne particulate matter PM<sub>10</sub>. (A) 12 different spots of PM<sub>10</sub> shows 12 different types of spectral  
685 peaks corresponding to presence of specific elements at that point. (B) Representation of elemental composition (%  
686 weight) of PM<sub>10</sub> at few other spots in bar graph having metal name on *y-axis* and respective concentration (%weight)  
687 on *x-axis*.

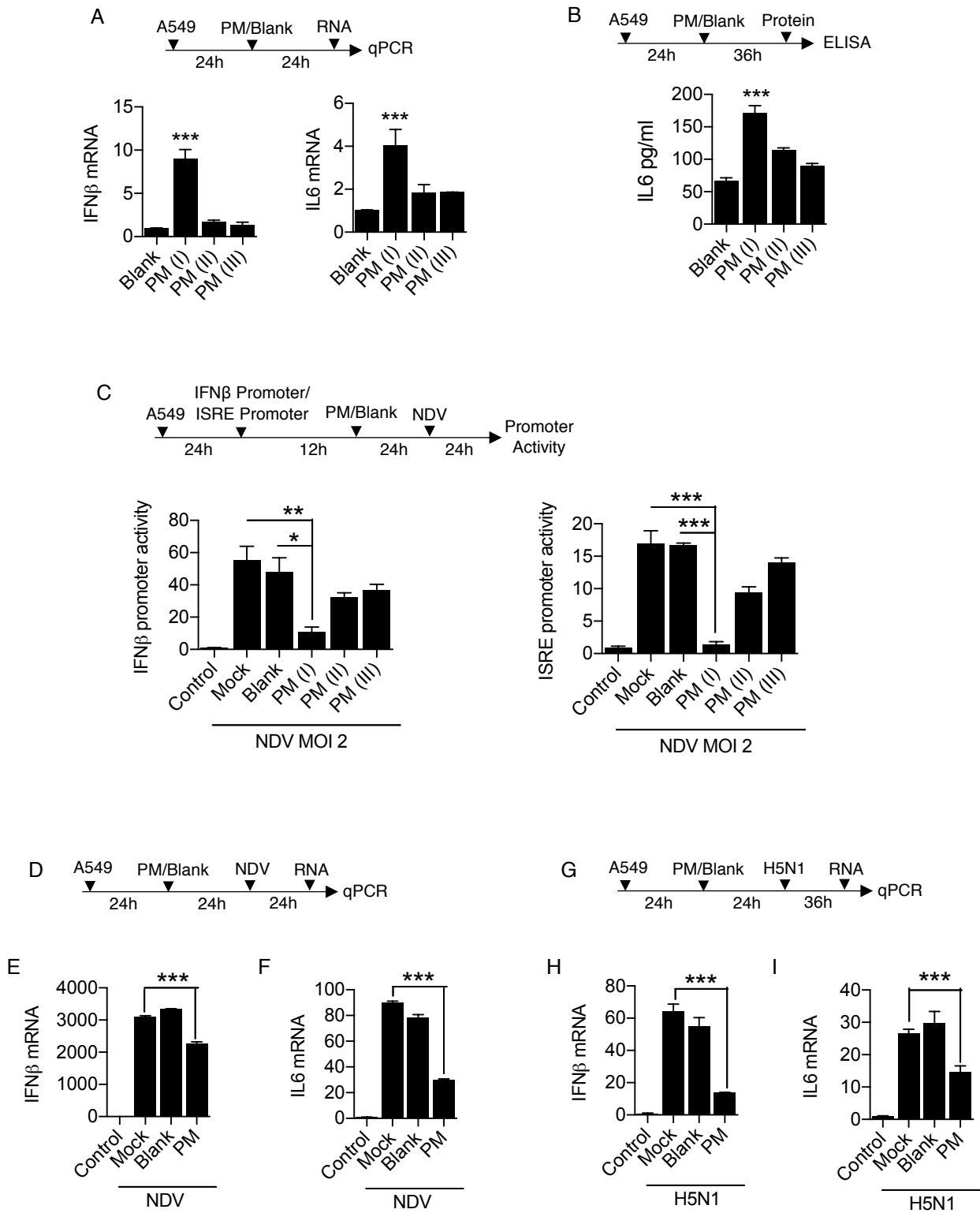
688 **Supplementary Figure 2: GEO dataset GSE27973 re-analysis** – (A) Cellular pathways dysregulated in presence  
689 of CSE (cigarette smoke extract) exposure and rhinovirus infection in human bronchial epithelial cells. (B) Number  
690 of genes involved in various diseases. (C) Exact gene plotted against the disease in which it is involved, represented  
691 in the heat map generated by the Enrichr software. (D) Connecting network between the pathways dysregulated,  
692 represented in the dot network analysis generated by the Enrichr software.

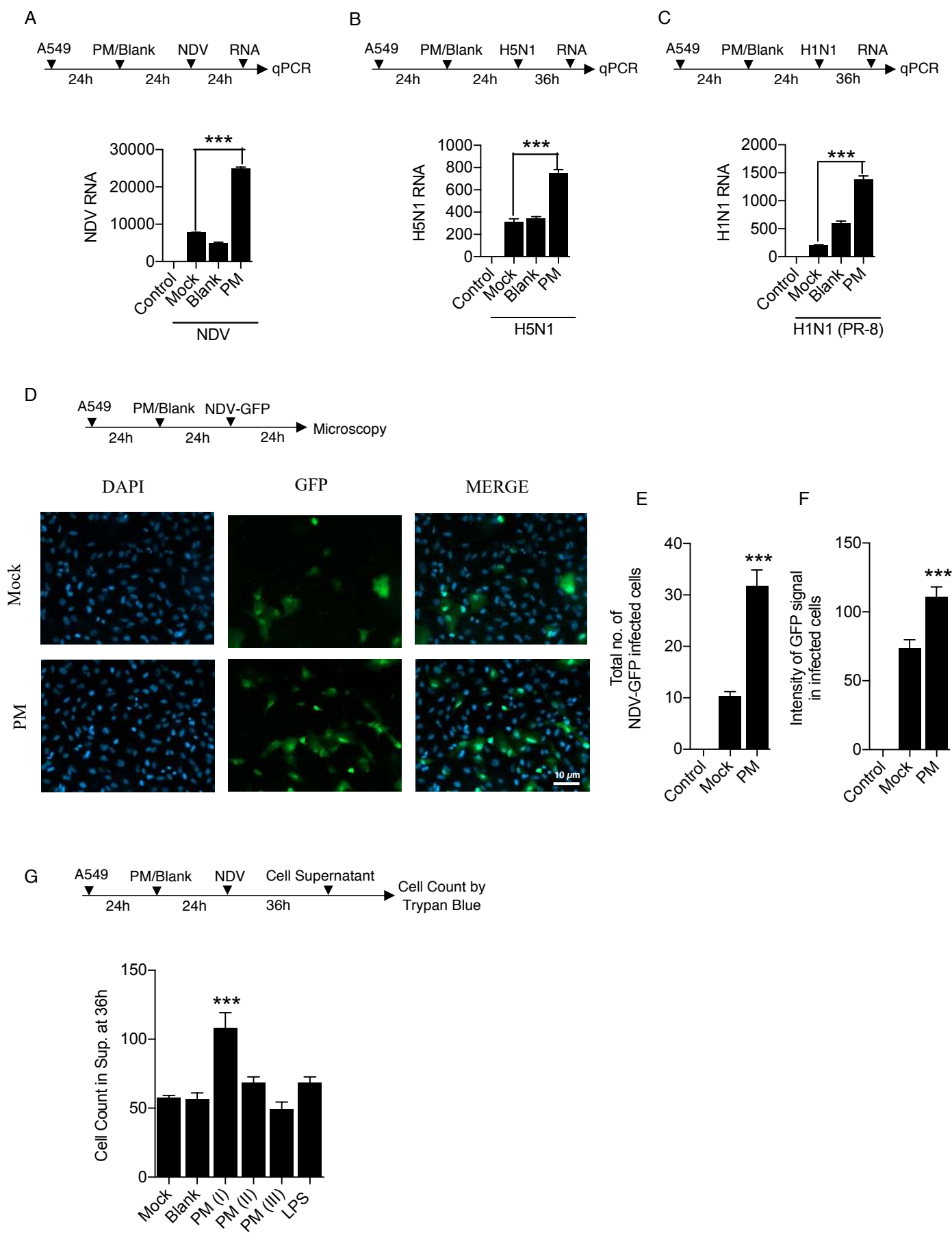
693 **Supplementary Figure 3: Gene Ontology analysis of PM<sub>10</sub> treated and H5N1 infected A549 cells** – (A) Gene  
694 Ontology analysis represented by the chord plot that connects the common differentially expressed genes with the top  
695 significantly enriched ontology terms. (B-E) Quantification (measured by qRT-PCR) of the fold changes in the  
696 abundances of metabolic pathways related transcripts: VIPR1, CYP1A1, ALDH1A3 and PPP1R14A in A549 cells  
697 exposed with PM<sub>10</sub> and infected with NDV. Sample labelled as untreated (control), mock NDV infected (NDV) and  
698 PM<sub>10</sub> exposed plus NDV infected (NDV+PM). Data are mean +/- SEM of triplicate samples from single experiment  
699 and are representative of two independent experiments. \*\*\* $P < 0.001$ , \*\* $P < 0.01$  and ns = non-significant by one-way  
700 ANOVA Tukey test and unpaired t-test.

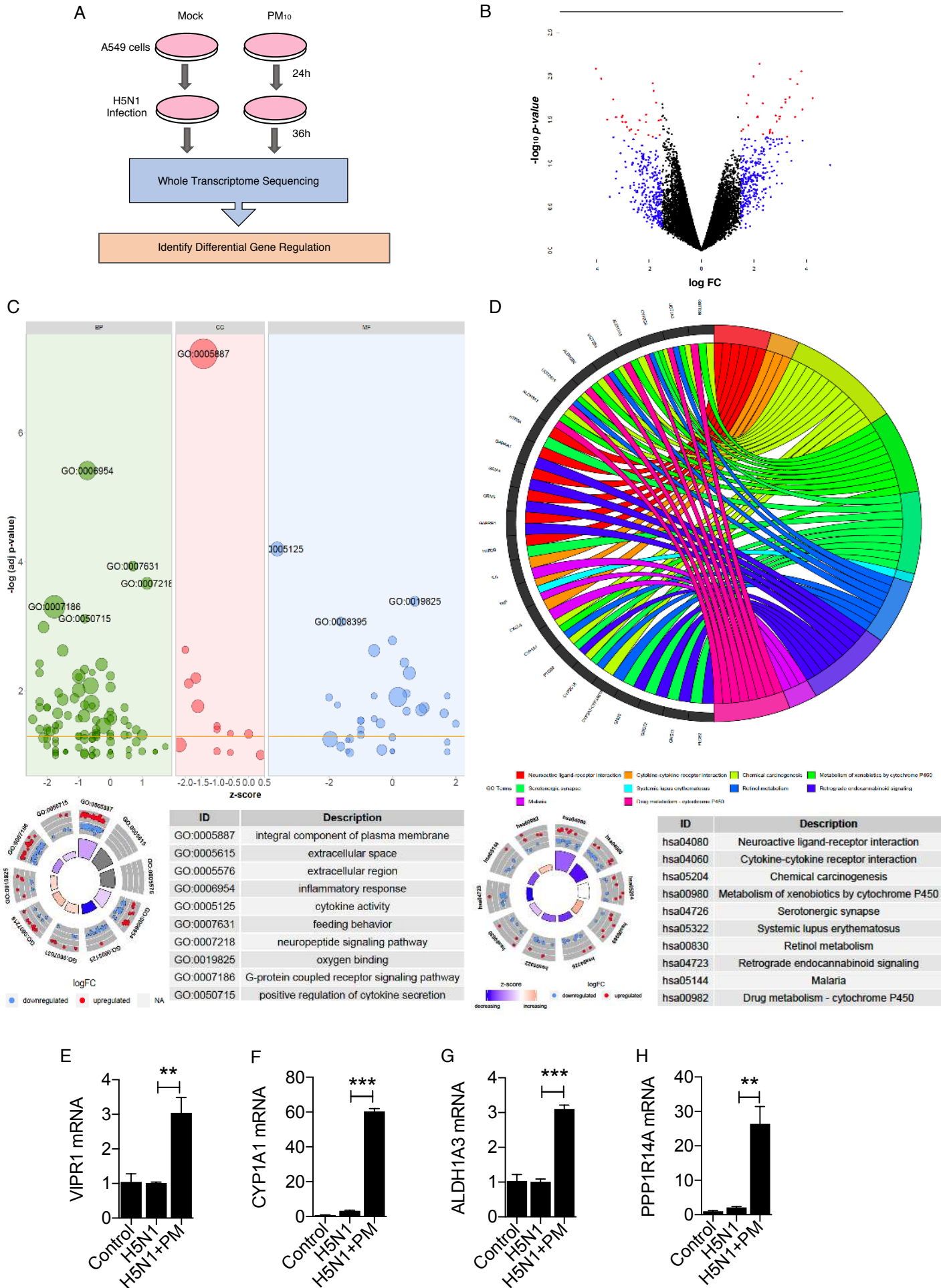
701 **Supplementary Figure 4: GEO dataset GSE27973 re-analysis to depict the pathways and genes upregulated in**  
702 **presence of CSE and RV infection** – Enrichr software is used for the depiction of related genes and pathways. (A)  
703 Representation of enriched pathways by bar graph. (B) Representation of upregulated genes involved in enriched  
704 pathways by heat map. (C) Representation of upregulated genes involved in various diseases by heat map. Here,  
705 human bronchial epithelial cell lines were exposed to CSE (cigarette smoke extract), RV (rhinovirus).





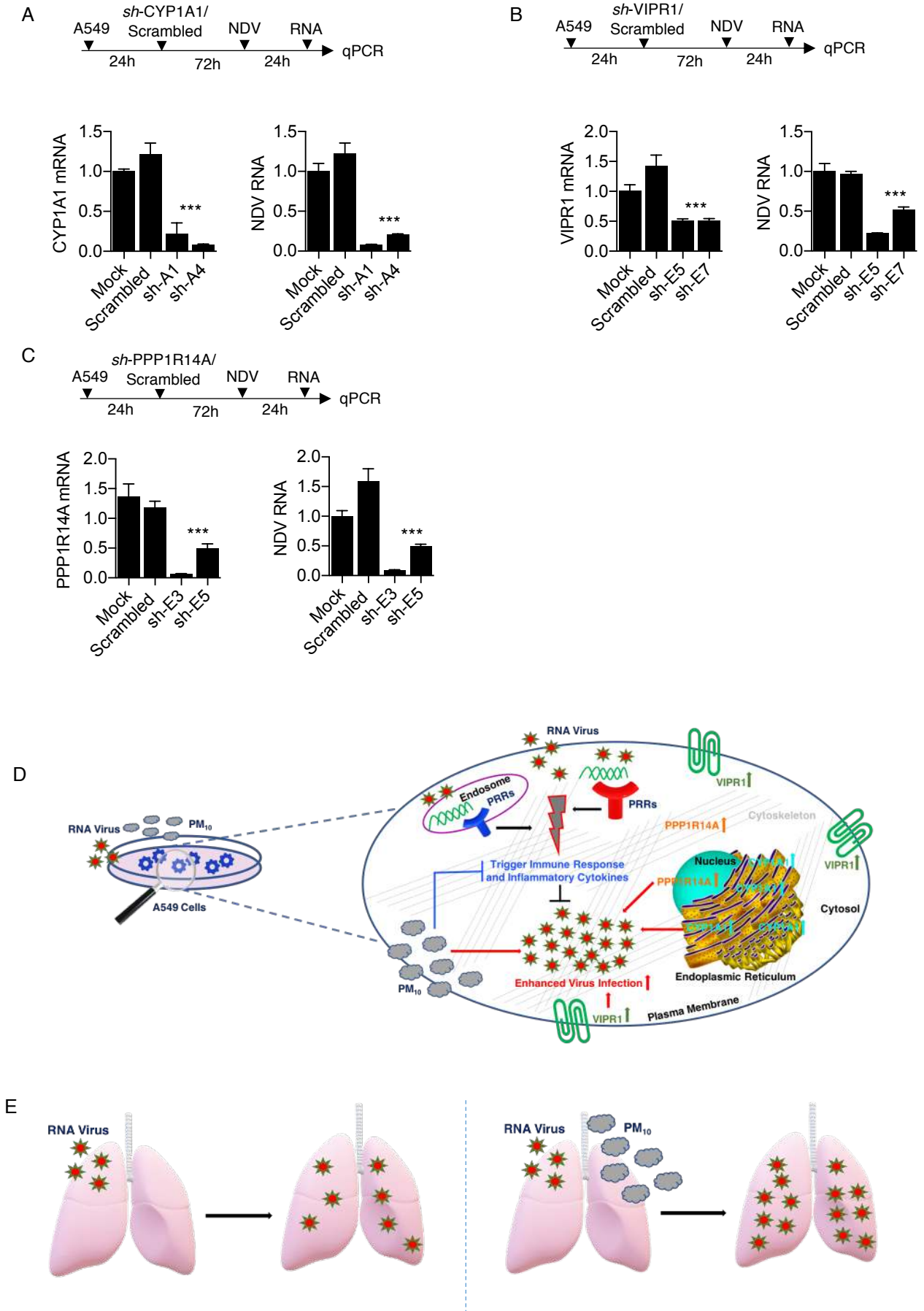


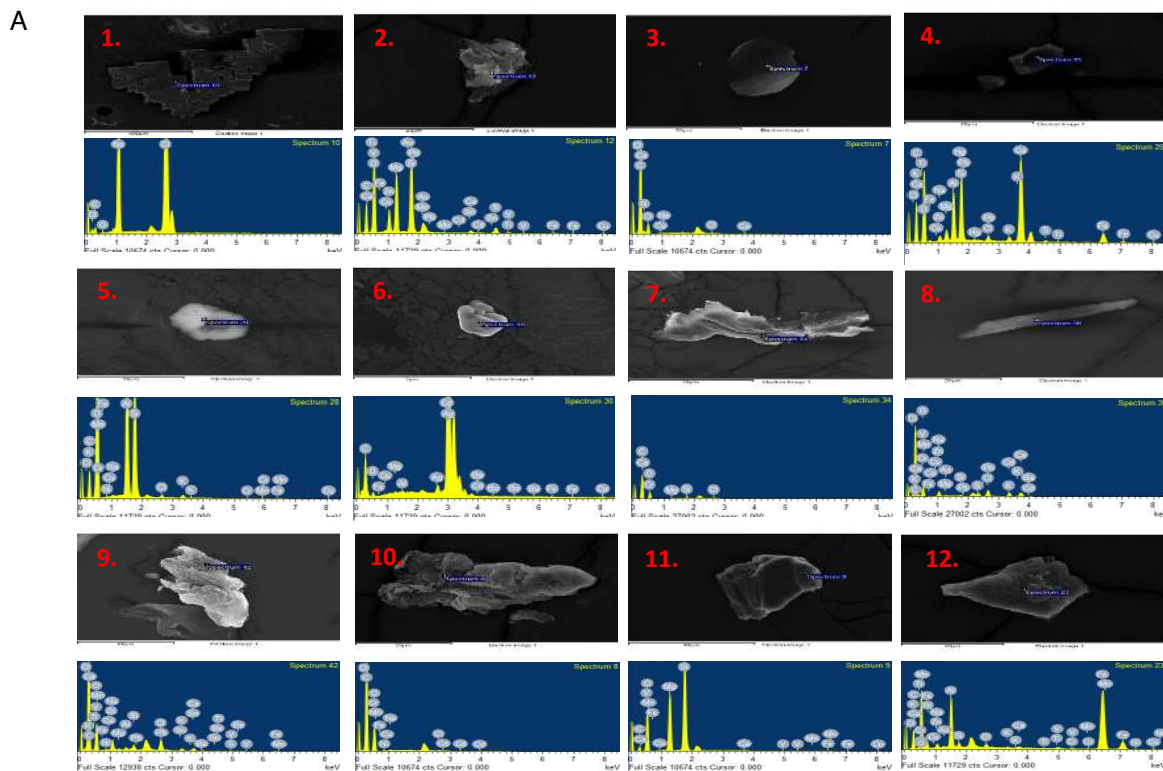




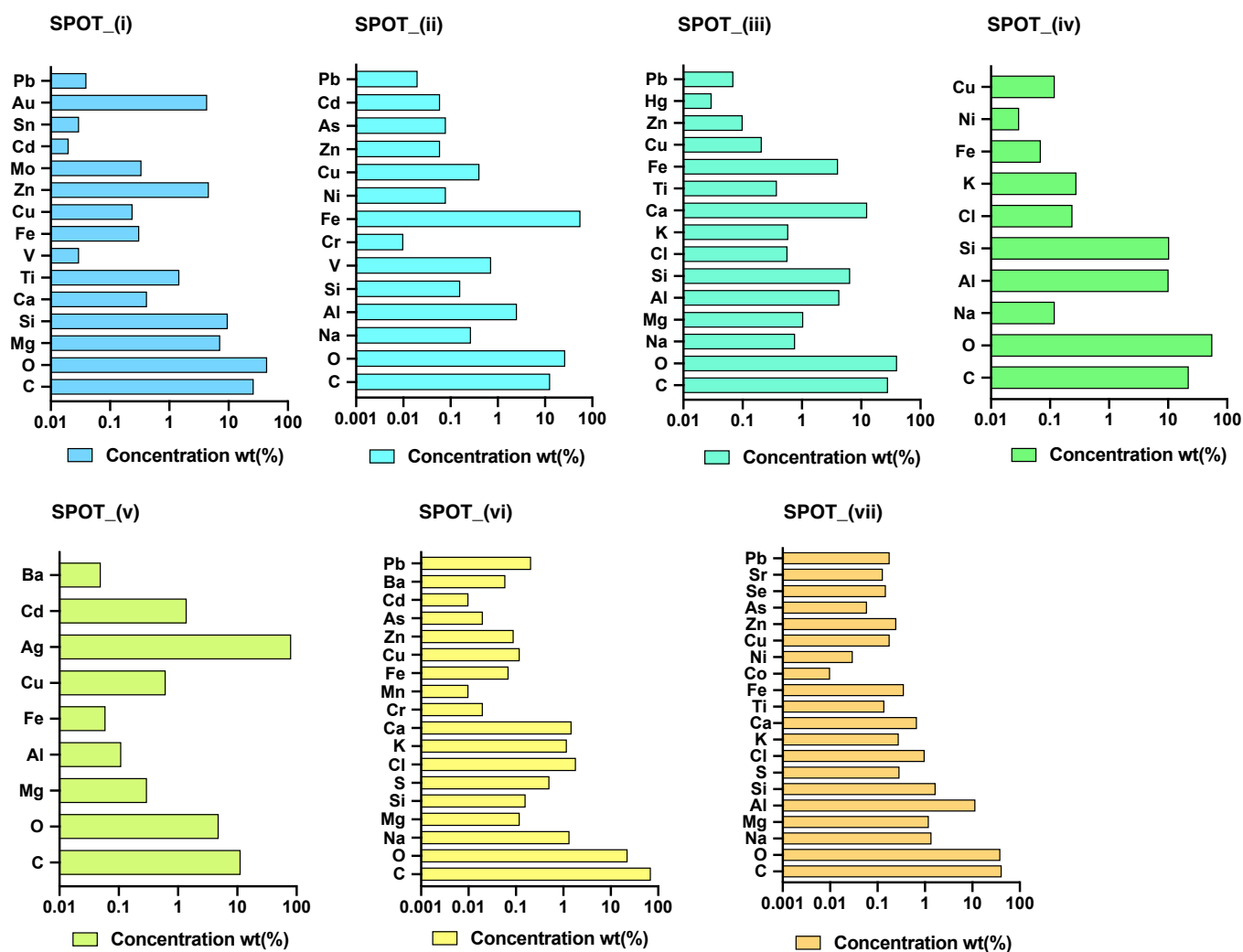


**Figure 5.**

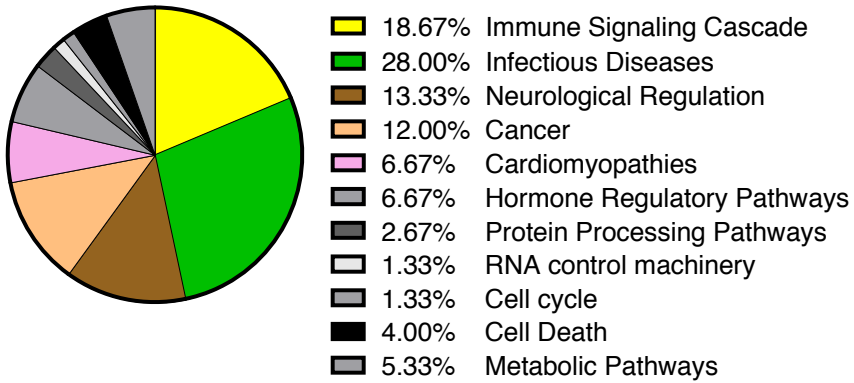




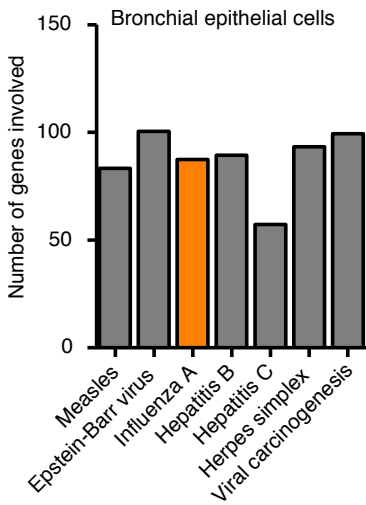
**B**



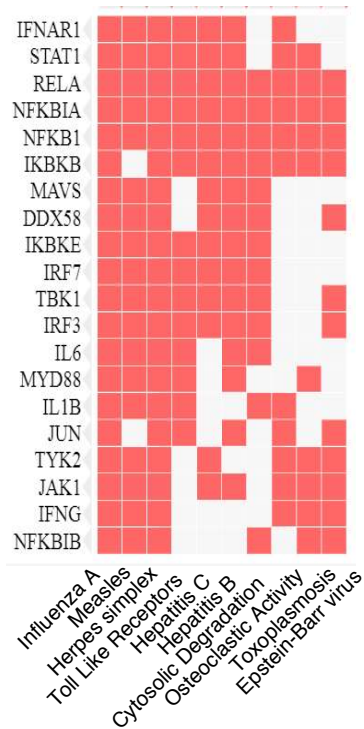
A



B



C



D

